Clinical Radiology (2000) **55,** 82–98
doi:10.1053/crad.1999.0328, available online at http://www.idealibrary.com on IDEAL®

Pictorial Review

Intra-Cranial Manifestations of the Neurocutaneous Syndromes

J. HERRON, R. DARRAH, G. QUAGHEBEUR*

*Department of Radiology, John Radcliffe Hospital, Headley Way, Headington, Oxford, OX3 9DU, *Department of Neuroradiology, Radcliffe Infirmary, Woodstock Road, Oxford, OX2 6HE, U.K.*

Received: 18 February 1999 Revised: 26 June 1999 Accepted: 9 July 1999

The neurocutaneous syndromes or phakomatoses are a heterogeneous group of congenital disorders primarily involving structures derived from the embryological neuroectoderm. All of the syndromes involve the central nervous system (CNS). Peripheral nerves, skin and other organ systems may also be involved. Twenty to 30 disorders are now classified as neurocutaneous syndromes. This article reviews the intra-cranial imaging features of some of the commonest. Herron, J. *et al*. (2000). *Clinical Radiology* **55**, 82–98.

Key words: neurocutaneous, central nervous system, imaging features.

NEUROFIBROMATOSIS

First described over 100 years ago by Von Recklinghausen, it is now clear that there may be as many as eight different clinical subtypes. Types one and two (NF-1 and NF-2) account for over 99% of cases.

Neurofibromatosis Type 1 (Von Recklinghausen's Disease/'Peripheral' NF)

This disease is characterized by mutliple cutaneous skin lesions, CNS tumours and mesoderm dysplasia. It is autosomal dominant with an incidence of one in 3000 and is due to a mutation of chromosome 17. It has a high penetrance with variable expressivity but about 50% of patients have mutations with no family history. It is not an absolute clinical entity and up to seven forms may exist. CNS findings include both neoplastic lesions and harmartomas [1,2].

The incidence of CNS manifestations in NF-1 is 15–20%, and there is a four-fold increased risk of developing a CNS neoplasm as compared to the general population.

Intracranial Manifestations

Optic pathway gliomas are the most common brain abnormality in NF-1 and occur in 30% of cases. These tumours appear as either a focal mass on the optic nerve or as a diffuse enlargement of a long segment [2]. T2W MRI may show high signal (thought to be posterior extension) in the optic chiasm, tracts and radiations (Figs 1, 2).

These gliomas are most commonly juvenile pilocytic astrocytomas, but other low and higher-grade gliomas occur. The mesencephalic tectum is the commonest site after the optic pathways, and lesions also occur in the brainstem and cerebrum (Figs 3, 4). Hydrocephalus is not uncommon and may result either from benign acqueductal stenosis or gliomas of the tectum or tegmentum.

Characteristic foci of increased signal intensity are present in about 75% of patients with NF-1. These lesions are usually multiple, show no mass effect or contrast enhancement, and elicit no oedema. They are commonest in the pons, cerebellar white matter, internal capsule and splenium (Figs 1, 4). They tend to appear at age 3 years, increasing in size and number till age 10/11 years, and then progressively disappear. They are though to represent harmartomas, abnormal glial cells or dysplastic myelination. Follow-up MRI is recommended to differentiate these lesions from low-grade neoplasms [4]. Similar foci of altered signal are seen in globus pallidus, and although these may show a little mass effect and slight hyperintense signal on T1W MRI they are also presumed to be hamartomas [1,5].

Other abnormalities include cranial nerve tumours (rarely); bone dysplasias such as sphenoid wing hypoplasia with subsequent pulsating exopthalmos (Fig. 5); plexiform neurofibromas (Fig. 5); and orbital abnormalities such as bupthalmos (enlargement of the globe due to congenital glaucoma), retinal phakomas and Lisch nodules.

Correspondence to: Dr J. Herron, Specialist Registrar Radiology, Department of Radiology, John Radcliffe Hospital, Headley Way, Headington, Oxford OX3 9DU, U.K.
Guarantor of study: Dr G. Quaghebeur.

0009-9260/00/020082+17 $35.00/0

(*a*)

(*b*)

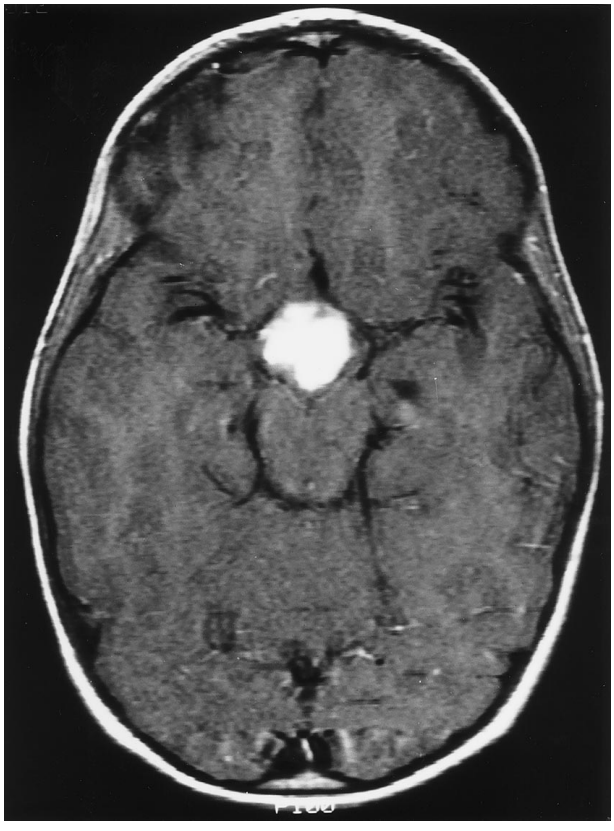

(*c*)

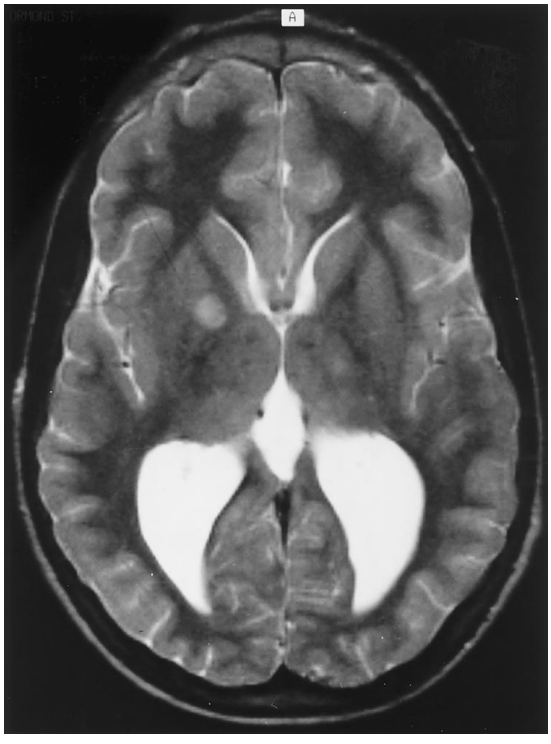

(*d*)

Fig. 1 – A 14-year-old patient with NF-1. (*a*) MRI (T2-weighted axial with fat saturation) shows bilateral optic nerve gliomas. These are seen as diffuse enlargement of the nerves. These are seen in 10–70% of patients. (*b*) MRI (T2-weighted axial) shows a bulky chiasm and a lesion in the cerebral peduncle representing a probable hamartoma. (*c*) MRI (enhanced T1-weighted axial) shows high signal within the chiasmatic tumour. (*d*) MRI (T2-weighted axial) shows high signal within the basal ganglia and the cerebral peduncles. These are seen in 75% of patients and are thought to represent hamartomas, abnormal glial cells or dysplastic myelination.

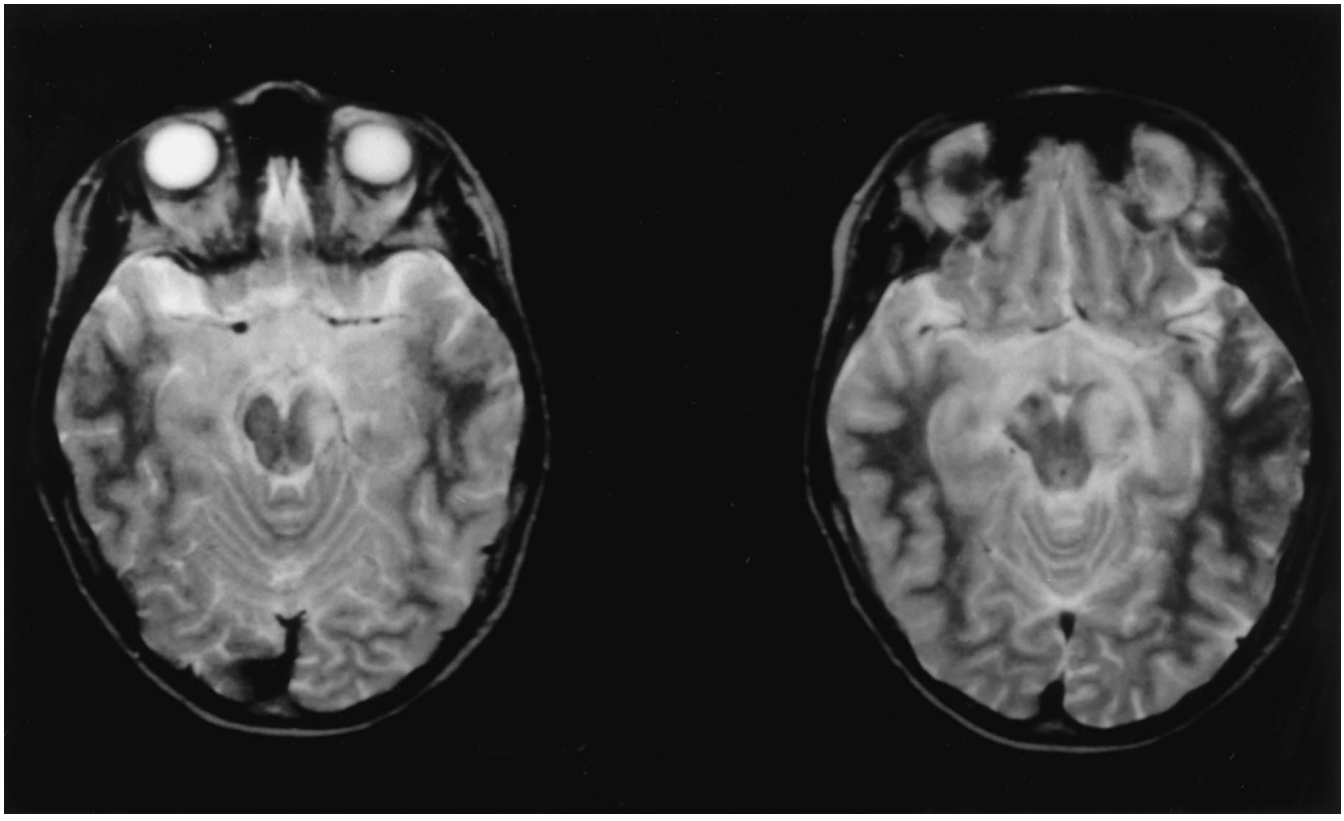

(*a*)

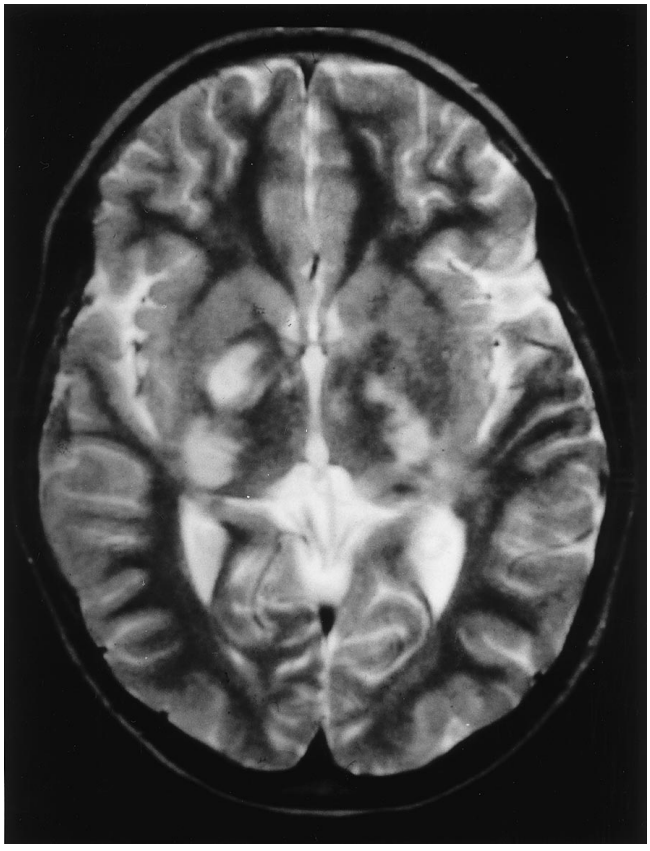

(*b*)

Fig. 2 – An 8-year-old patient with NF-1. (*a*, *b*) MRI (T2-weighted axial) shows high signal within the optic tracts and radiations due to posterior extension of an optic chiasm glioma, (*c*) MRI (enhanced T1-weighted coronal) shows high signal within the optic radiations, and an intraventricular glioma.

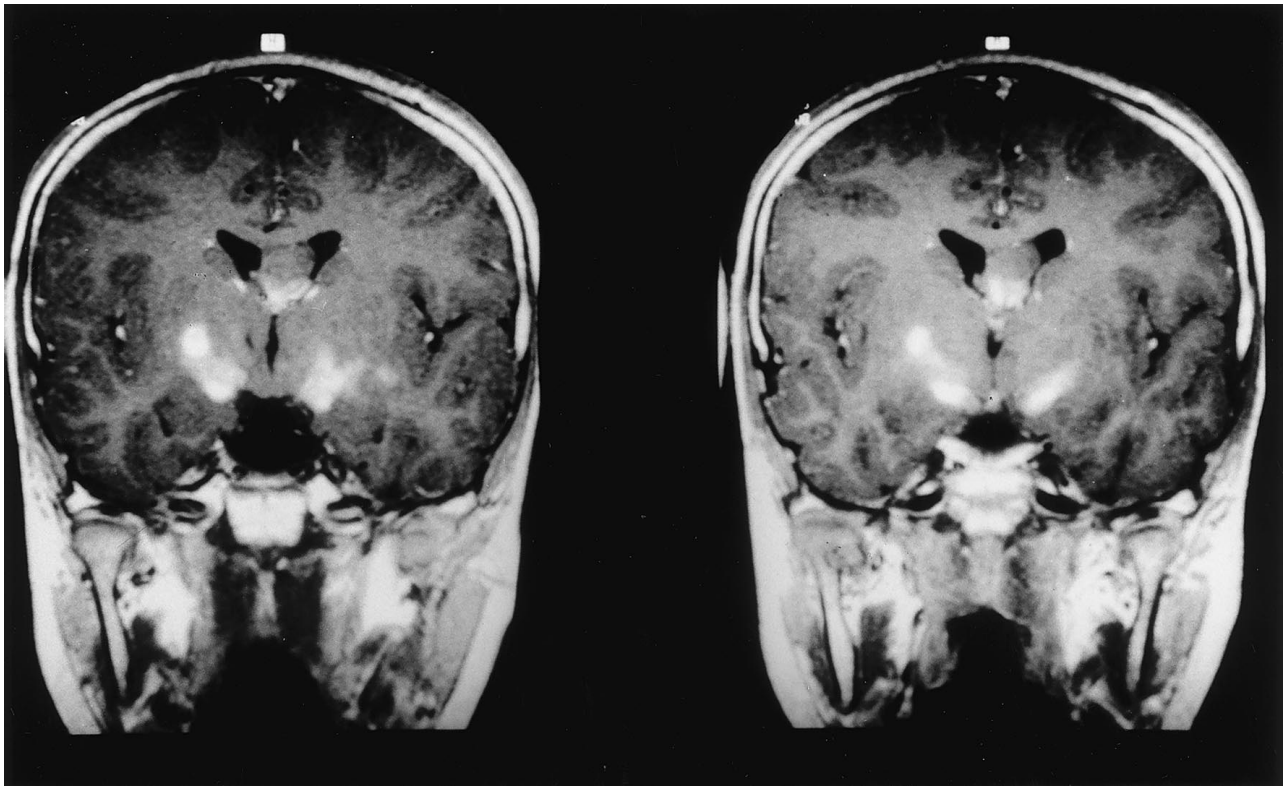

(*c*)

Fig. 2 – continued.

Vascular dysplasias due to intimal proliferation can result in stenoses and occlusions. Aneurysms and arterio-venous malformations (AVM) are also described (Fig. 6).

Neurofibromatosis Type 2

This disorder is characterized by bilateral vestibular schwannomas. NF-2 is associated with a deletion on chromosome 22, is autosomal dominant and has an incidence of one in 50 000. Cutaneous manifestations are rare.

Intracranial Manifestations

The characteristic lesions are schwannomas of the acoustic and other cranial nerves (particularly V, sometimes X), and meningiomas. The neoplasms tend to arise from the coverings of the brain (Figs 7–10).

The bilateral vestibular schwannomas (Fig. 10) present in the second and third decade. They may be cystic.

Meningiomas are often multiple and intraventricular and tend to calcify. They are particularly seen in the lateral ventricle. The choroid plexus may enlarge and become calcified (Fig. 10).

Other Forms of Neurofibromatosis

Some patients have a syndrome that appears to be an overlap of NF-1 and NF-2, and this NF-3 syndrome is now recognized clinically although the genetics are not fully established.

Table 1 – Diagnostic criteria for NF-1 requires two or more of the following [3]:

Symptom
Six or more *café au lait* spots; >5 mm before puberty, >15 mm after puberty
One plexiform, or two ordinary neurofibromas
Two or more lisch nodules (pigmented iris hamartomas)
Axillary or inguinal freckling
Optic nerve glioma
First degree relative with NF-1
One or more distinctive bone lesions, e.g. sphenoid dysplasia, pseudoarthrosis, thinning of a long bone cortex

Several other forms of neurofibromatosis have also been described by Riccardi, all of which may present with intracranial lesions [6].

TUBEROUS SCLEROSIS (BOURNEVILLE'S DISEASE)

Tuberous sclerosis (TS) is a familial multisystem disease. It is an autosomal dominant disorder with low penetrance, variable expressivity and a prevalence of one in 34 000–100 000 [1,7]. It has been linked to an abnormality on chromosomes 9 and 16 [7]. The classic triad of symptoms described by Volt in 1908 of seizures, mental retardation and adenoma sebaceum is one end of a clinical spectrum and is seen in less than one-third of cases [2]. Criteria for the diagnosis of this disorder have now been established [1]. Radiological criteria are important in establishing this diagnosis and may be manifest earlier than some clinical features [7].

Intracranial Manifestations

TS derives its name from the cortical hamartomas or tubers seen in the gyri (most commonly of frontal lobe). These lesions are seen in 95% of cases. Some calcify although the proportion that does so has not been established. The number of calcified cortical lesions increases with age, by age 10 50% of TS patients have calcified cortical tubers. On CT the tubers may appear as lucencies in widened gyri in young patients, this becomes more difficult to see with age unless the lesions calcify. MRI detects these lesions well at all ages, again the features change with age (Fig. 11). In neonates, the gyri appear enlarged and hyperintense to the surrounding unmyelinated white matter on T1W images and hypointense to the white matter on T2W MR images. As the white matter myelinates the appearance alters and the lesions are hypointense on T1W and hyperintense on T2W MR, ultimately becoming isointense on T1W images with increasing age. As the lesions calcify they may again show some T1 hyperintensity [1].

Subependymal nodules or hamartomas are seen in 90% of cases. The majority calcify and are typically found along the ventricular surface of the lateral ventricle in the striothalamic groove between the caudate and the thalamus, just posterior to the foramen of Munro. Less often, they are seen elsewhere in the ventricular system. The imaging characteristics on CT and MR alter with age, showing progressive calcification on CT. On MR, the nodules alter in signal intensity as myelination progresses. They are best seen on T1W MR images. They may show enhancement with intravenous GdDTPA (Fig. 11).

Giant cell astrocytomas occur in up to 15% of TS patients. They occur at the foramen of Munro and present as enlarging partly calcified masses with associated hydrocephalus (Fig. 12). Serpentine flow voids due to dilated vessels are seen in one-third. Their appearance varies and neither signal intensity or contrast enhancement can differentiate the tumour from a subependymal nodule – the change in size is most important. Histologically these tumours tend to be astrocytomas.

White matter lesions are seen in 90% of cases. Many of these represent islets of disordered neurones and glial cells. In a recent study, 21% of patients [9] showed linear or curvilinear hyperintensities in the white matter, extending from subependymal nodules to cortical tubers. These are thought to be bands of hypomyelinated disordered or gliotic cells along the linear radial glial-neuronal unit.

Cerebellar white matter lesions occur in 10% of patients.

STURGE WEBER SYNDROME (ENCEPHALOTRIGEMINAL ANGIOMATOSIS)

This is a congenital disorder of vasculature of the face, the choroid of the eye, and the leptomeninges. It occurs sporadically affecting both sexes equally, but familial cases are reported. The facial angioma (port wine naevus) can involve all or part of the face and is present at birth. It does not change with age. In some cases of SWS there is no facial angioma [1]. The original description by Schirmer in 1860 of a naevus in the distribution of the trigeminal nerve with an ipsilateral leptomeningeal abnormality in the occipital region is not characteristic.

The major pathologic abnormality in SWS is a meningeal angioma in the pia mater, possibly due to persistent primordial sinusoidal vascular channels. This leads to a lack of superficial cortical venous drainage resulting in chronic venous hypertension and ischaemia [1,10].

Intracranial Manifestations

The leptomeningeal vascular malformation is best seen on contrast-enhanced MRI (Fig. 13). Other MR findings include low signal on T2W of the affected gyri and adjacent white matter. The aetiology of this signal change is unclear and may be due to calcification, accelerated myelination or increased deoxyhaemoglobin in the capillaries and veins. Many of the other radiological findings result from the venous stasis. These include atrophy of the underlying cortex accompanied by cerebral calcification which is seen from 1 year of age (Fig. 14). The calcified opposed gyri are seen as parallel tram-track calcification on plain film.

Enlargement and calcification of the choroid plexus (Fig. 13) on the affected side is well documented, and the size of the choroid plexus correlates positively with the extent of leptomeningeal enhancement [11].

Enlarged vessels can be seen on MRI and CT deep in the hemisphere probably due to enlargement of deep venous vessels as a result of slow flow or thrombosis in the superficial abnormal venous system, and subsequent shunting of blood through deep medullary veins.

Cranial asymmetry can occur due to hemiatrophy, or paradoxically there may be a large hemicranium on the side of the atrophy secondary to associated subdural collections. The Dyke-Davidoff-Maison syndrome is a constellation of calvarial changes which is sometimes seen. It includes skull thickening, pneumatization of the paranasal sinuses, ipsilateral shift of the falx and elevation of the petrous ridge and lesser wing of sphenoid. This picture may also occur with other causes of hemicerebral atrophy [1].

VON HIPPEL-LINDAU SYNDROME

An autosomal dominant disorder with incomplete penetrance and a genetic defect at chromosome 3p25-p26 [1].

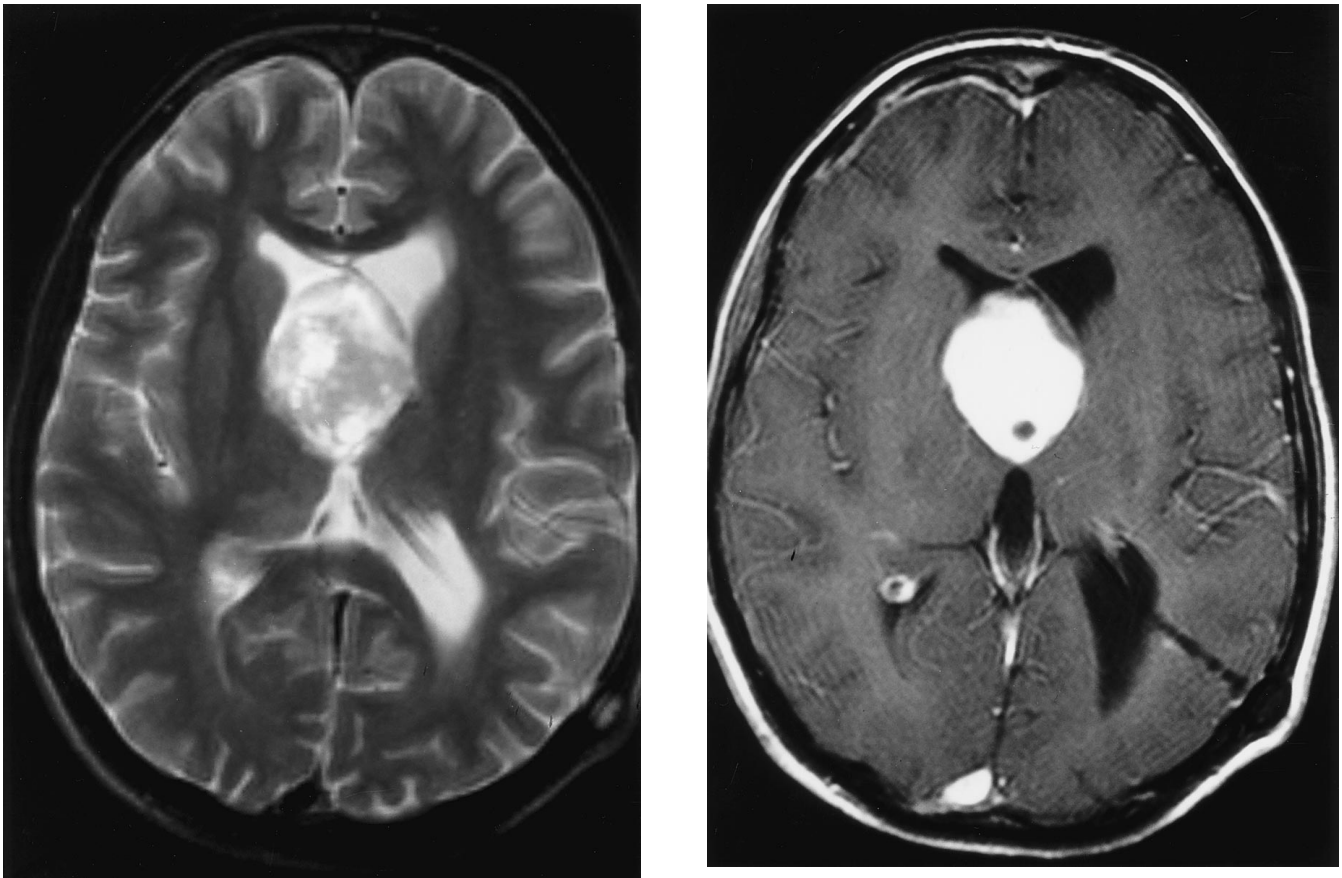

(*a*) (*b*)

Fig. 3 – A 20-year-old patient with NF-1. (*a*) MRI (T2-weighted axial) shows a glioma of the septum pellucidum. Although optic nerve gliomas are the most common glioma found in NF-1, gliomas do occur in the brain stem and cerebrum. (*b*) MRI (enhanced T1-weighted axial) shows avid enhancement of the glioma.

It is characterized by tumours of the CNS, typically multiple haemangioblastomas and tumours of the abdominal viscera. The haemangioblastomas occur primarily in the cerebellum (65%) brain stem (20%) and spinal cord (15%) [4]. They tend to be sharply demarcated with smooth borders. Two thirds of these lesions are cystic with a solid component or mural nodule [13] (Fig. 15). The nodule is isointense to brain on T1W MRI and hyperintense on T2W MRI. Flow voids within the nodule due to tumour vessels are common. The cystic component is hyperintense to CSF on T2W MRI and the wall of the cyst rarely enhances. The mural nodule enhances avidly. Solid tumours have intermediate to high signal on T2W MRI and enhance homogenously. Small areas of increased signal on T2W MRI in the white matter are sometimes seen. The exact nature of these lesions is unclear, they may represent subclinical haemangioblastomas, areas of gliosis or dystrophic white matter.

Many other disorders are now classified as neurocutaneous syndromes, however the vast majority of cases continue to be due to above five conditions. MRI is invaluable in diagnosis and shows previously unsuspected lesions. It is helping to increase our understanding of this complex and diverse group of disorders.

The issue of screening or long-term follow-up in patients with these syndromes is as yet unresolved. In 1988 Roach [14] addressed the use of screening for neurofibromatosis, but there is no more recent work. He recommended annual 'follow-up' of these patients, much of which can be clinical or electrophysiological. MRI is now a useful and acceptable tool and it is the practice in our department to examine these patients yearly.

If patients develop new or altered symptomatology, imaging is obtained as appropriate. Genetic assessment and counselling is vital, and may recommend screening of asymptomatic relatives. Griffiths [7] states that diagnosis of TS is readily made on CT imaging although MRI is more sensitive and may be useful for prognosis. Interval imaging to detect change on SENs and the development of giant cell astrocytoma is of limited value, as patient symptomatology determines whether any intervention is needed. Clinical examination of relatives is only minimally less sensitive than radiological screening and far more cost-effective. In VHL patients, screening on an annual basis has been recommended by several groups [12] and this includes enhanced MRI of brain and spine and abdominal CT or ultrasound. The latter is recommended to allow early detection of the potentially life threatening renal

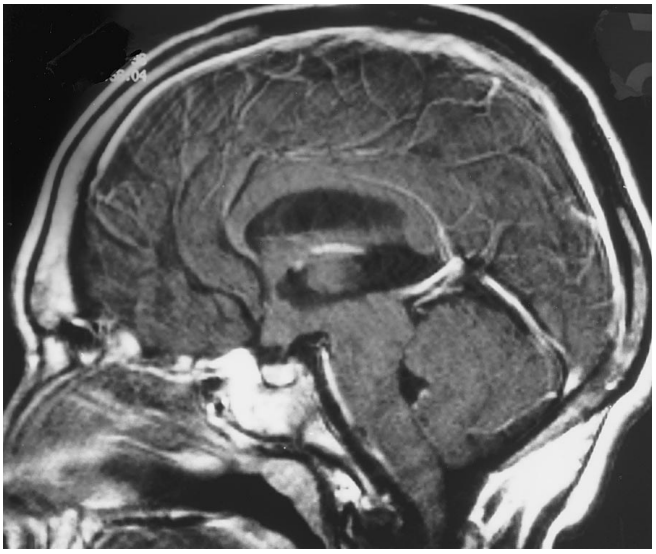

(*a*)

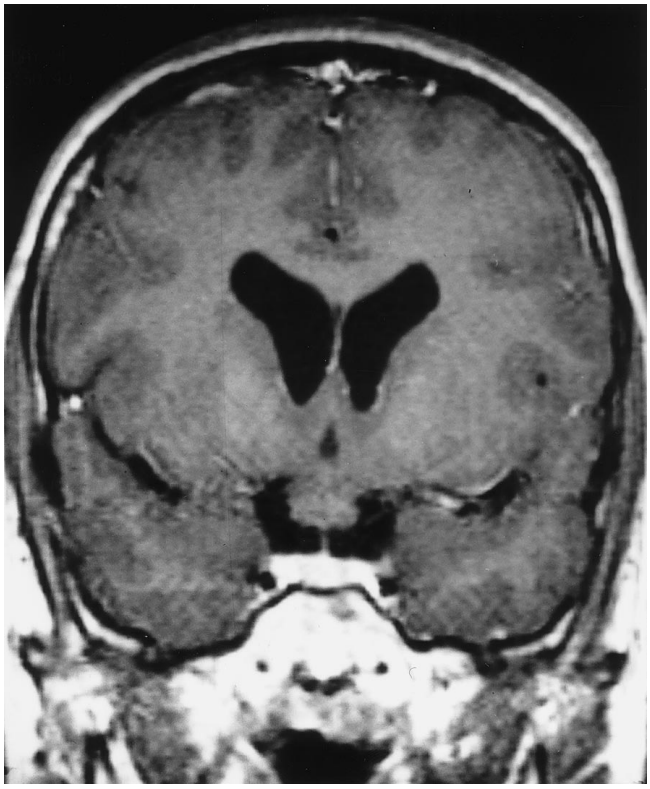

(*b*)

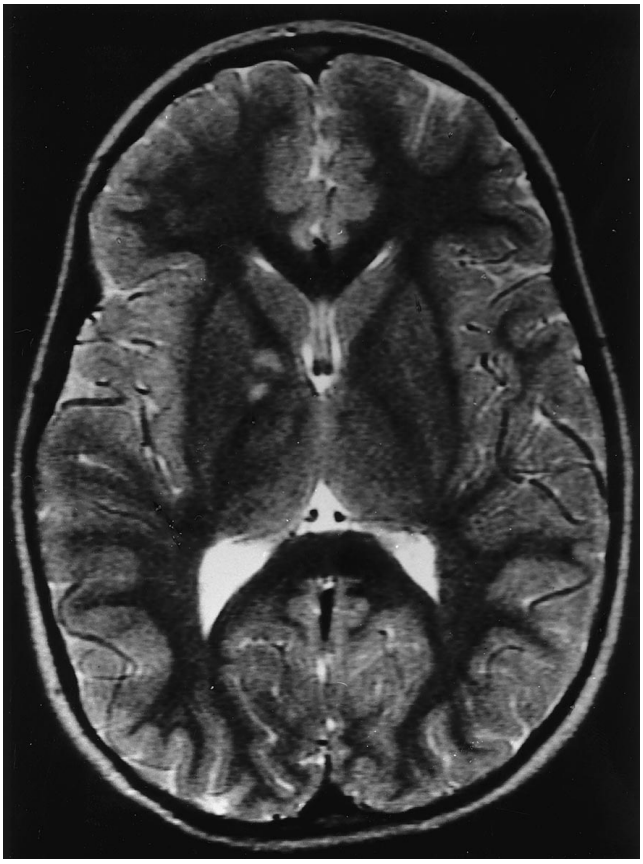

(*c*)

Fig. 4 – A 12-year-old patient with NF-1. (*a*) MRI (enhanced T1-weighted sagittal) shows a tectal plate glioma. (*b*) MRI (enhanced T1-weighted axial) shows a chiasmatic glioma. (*c*) MRI (T2-weighted axial) shows high signal in the putamen on the right.

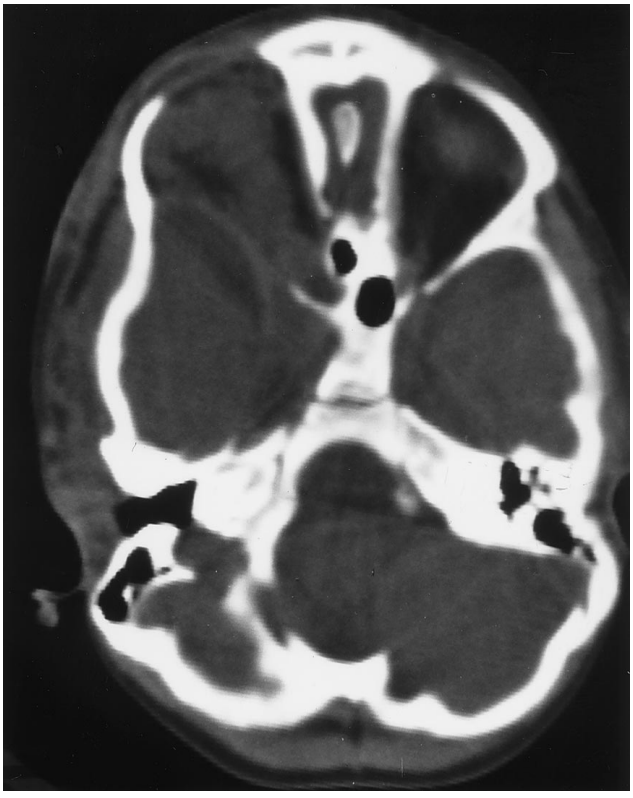

(*a*)

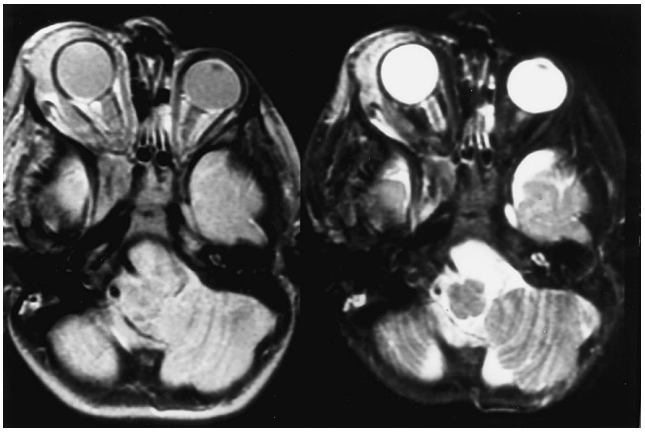

(*b*)

Fig. 5 – A 6-year-old patient with NF-1. (*a*) CT showing sphenoid wing dysplasia. This is associated with pulsating exopthalmos. (*b*) MRI (T2-weighted axial) shows the plexiform neurofibroma of the right orbit.

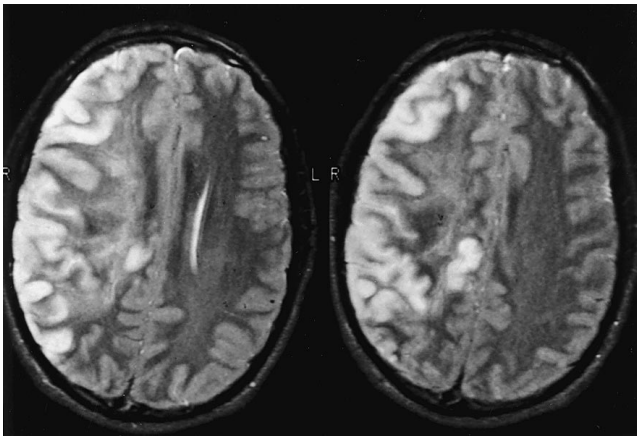

(*a*)

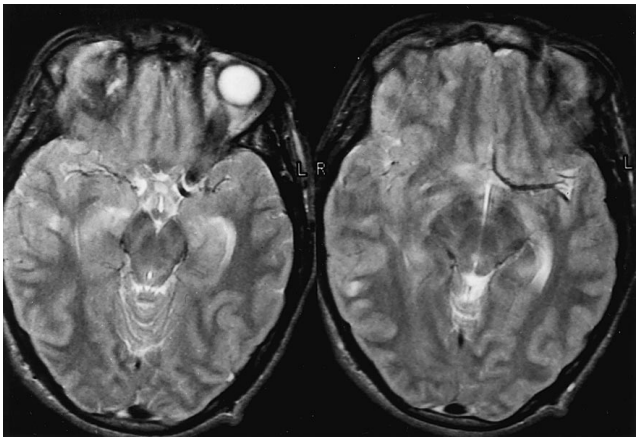

(*b*)

(*c*)

Fig. 6 – An 18-year-old patient with NF-1. (*a*) MRI (T2-weighted axial) shows right sided neurogenic oedema due to infarction. (*b*) MRI (T2-weighted axial) shows the absence of flow void in the right middle cerebral artery. (*c*) MR angiogram shows absence of signal from the right internal carotid artery.

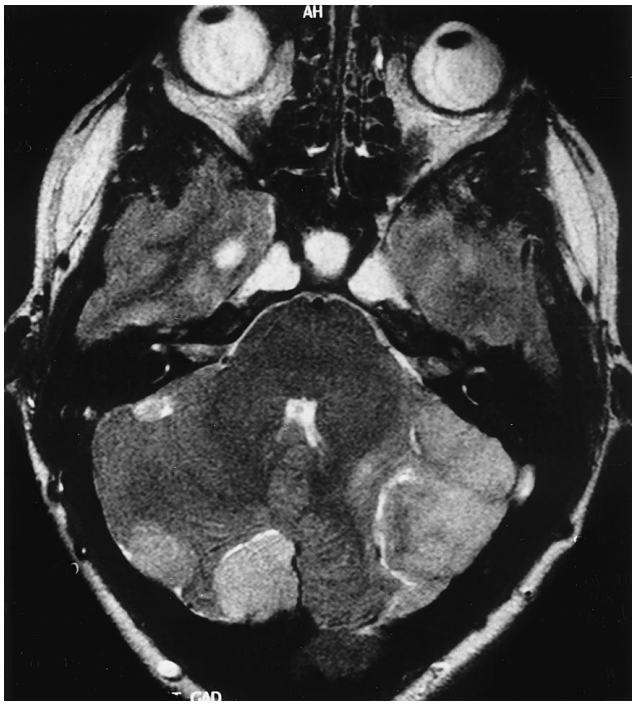

(*a*)

(*b*)

Fig. 7 – A 23-year-old patient with NF-2. (*a*) MRI (T2-weighted axial) shows multiple meningiomata in the posterior fossa. (*b*) MRI (enhanced T1-weighted axial) shows the meningiomata enhancing brightly.

Table 2 – Diagnostic criteria for NF-2 are [3]:

Criteria
Bilateral VIII nerve masses
A first-degree relative with NF-2 and either:
a. a unilateral VIII nerve mass
b. two of the following: meningioma, glioma, schwannoma, or juvenile posterior subcapsular lenticular opacity

and adrenal tumours. Asymptomatic relatives need careful genetic evaluation and dependant on the results of this, some will require annual screening also.

OTHER NEUROCUTANEOUS SYNDROMES

There are two main groups of disorders, the vascular and the melanocytic neurocutaneous syndromes. They include the following: (i) Wyburn-Mason syndrome. This comprises a facial vascular naevus and cerebral arteriovenous malformation which normally involves the visual pathway or the midbrain. The AVMs may be multiple (Fig. 16).

(ii) Ataxia telangiectasia. An autosomal recessive disorder with an incidence of one in 40 000 [1]. Oculocutaneous telangiectasia and cerebellar ataxia are seen. Cerebellar atrophy is seen affecting particularly the anterior vermis, with atrophy of the dentate and olivary nuclei and degeneration of the posterior columns (Fig. 17). Haemorrhage can result from rupture of parenchymal telangiectasia, and cerebral infarcts can result from emboli shunted through pulmonary vascular malformations. There is an increased incidence of lymphoma and leukaemia in this condition. (iii) Osler-Weber-Rendu disease (hereditary haemorrhagic telangiectasia). This autosomal dominant disorder presents with dermal, mucosal and visceral telangiectasia. Two-thirds have pulmonary arteriovenous fistulae. One-third have vascular malformations of the brain and spinal cord. Infarcts, septic emboli and abscess due to the complications of pulmonary fistulae are common. (iv) Klippel-Trenaunay-Weber syndrome. This consists of cutaneous angiomata, soft tissue or bony hypertrophy and a deep parenchymal vascular malformation. On MRI, vascular lesions, angiomas and hemimegalencephaly are all seen. (v) Meningioangiomatosis. This is part of a spectrum of hamartomatous meningeal-based lesions which involve the meninges, blood vessels and adjacent brain. The leptomeninges become thickened and on CT calcified lesions are seen. (vi) Neurocutaneous melanosis. One or more hairy or deeply pigmented naevi are seen in association with melanosis of the leptomeninges. Forty per cent develop primary melanosis of the CNS. CT is often normal, MR shows foci of altered T1 and T2 signal compatible with melanin deposition. Meningeal enhancement has been reported in some cases. (vii) Naevus of Ota syndrome. Blue grey lesions in the dermatomes of the ophthalmic and maxillary divisions of trigeminal nerve are associated with abnormal meningeal pigmentation, meningeal melanocytomas, melanomas of the choroid and ciliary body and primary melanomas of the CNS. (iix) Hypomelanosis of Ito. Hypopigmented skin

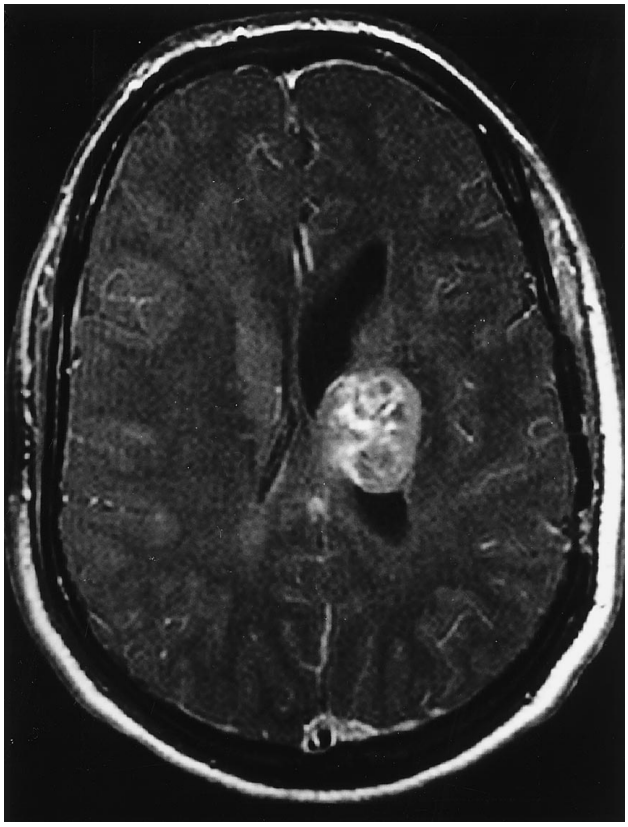

(*a*)

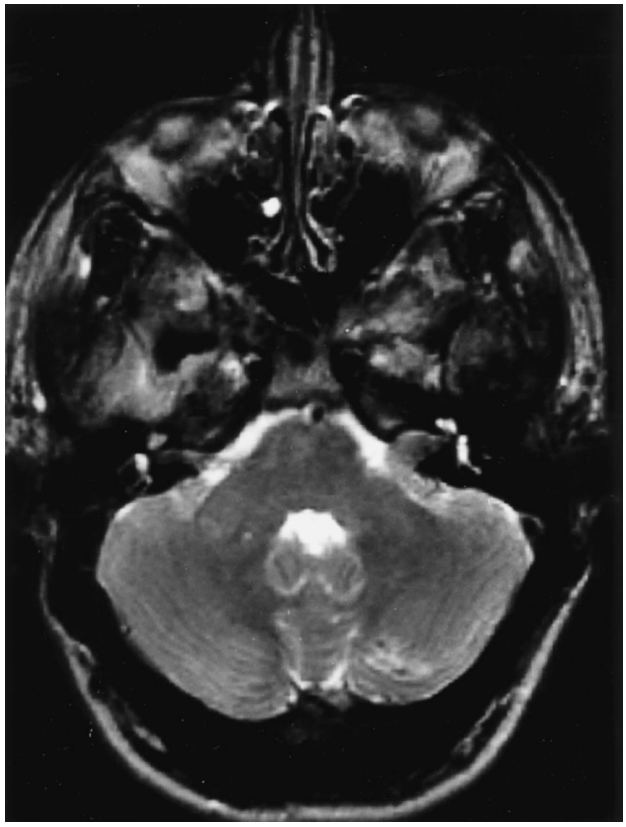

(*b*)

(*c*)

Fig. 8 – A 16-year-old patient with NF-2. (*a*) MRI (enhanced T1-weighted axial) shows an intraventricular meningioma. (*b*) MRI (T2-weighted axial) shows a left vestibular schwannoma. Note the enlargement of the internal auditory meatus. (*c*) MRI (T2-weighted axial) shows a schwannoma the left jugular foramen originating from either the X or XI cranial nerve.

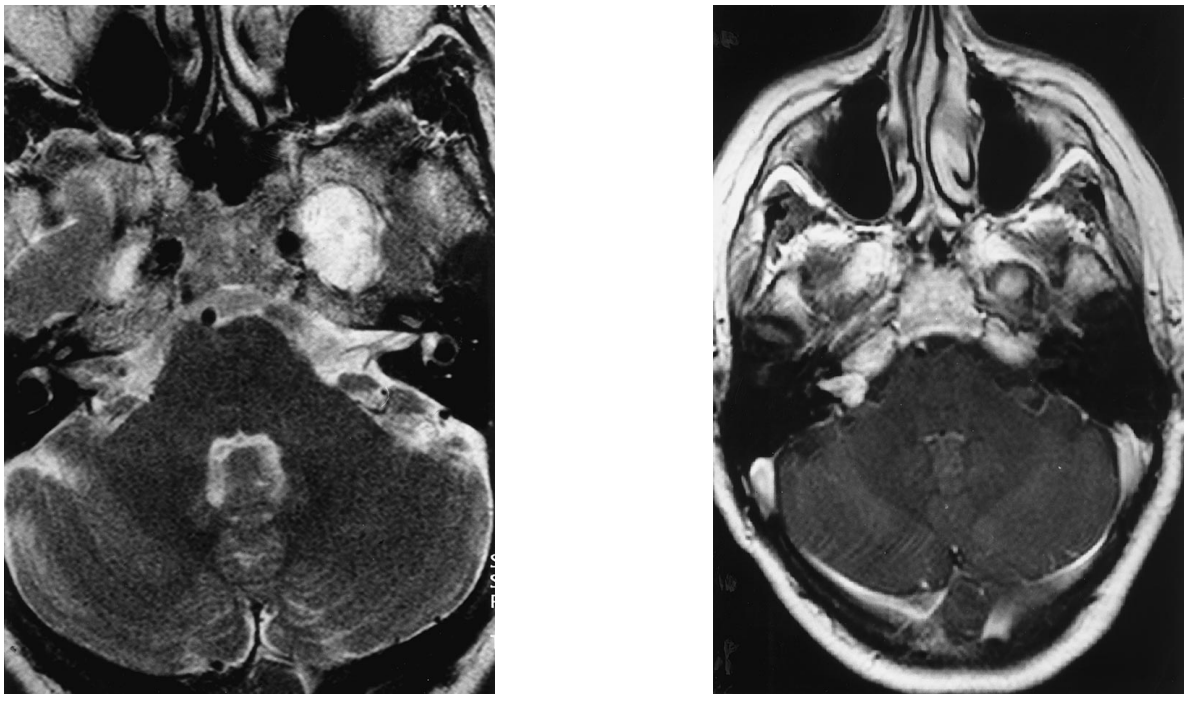

(*a*) (*b*)

Fig. 9 – A 27-year-old patient with NF-2. (*a*) MRI (T2-weighted axial) shows the VII and VIII nerves clearly in the left internal auditory meatus with CSF between them. On the right soft tissue is seen in this area. (*b*) MRI (enhanced T1-weighted axial) shows the vestibular schwannoma in the IAM enhancing.

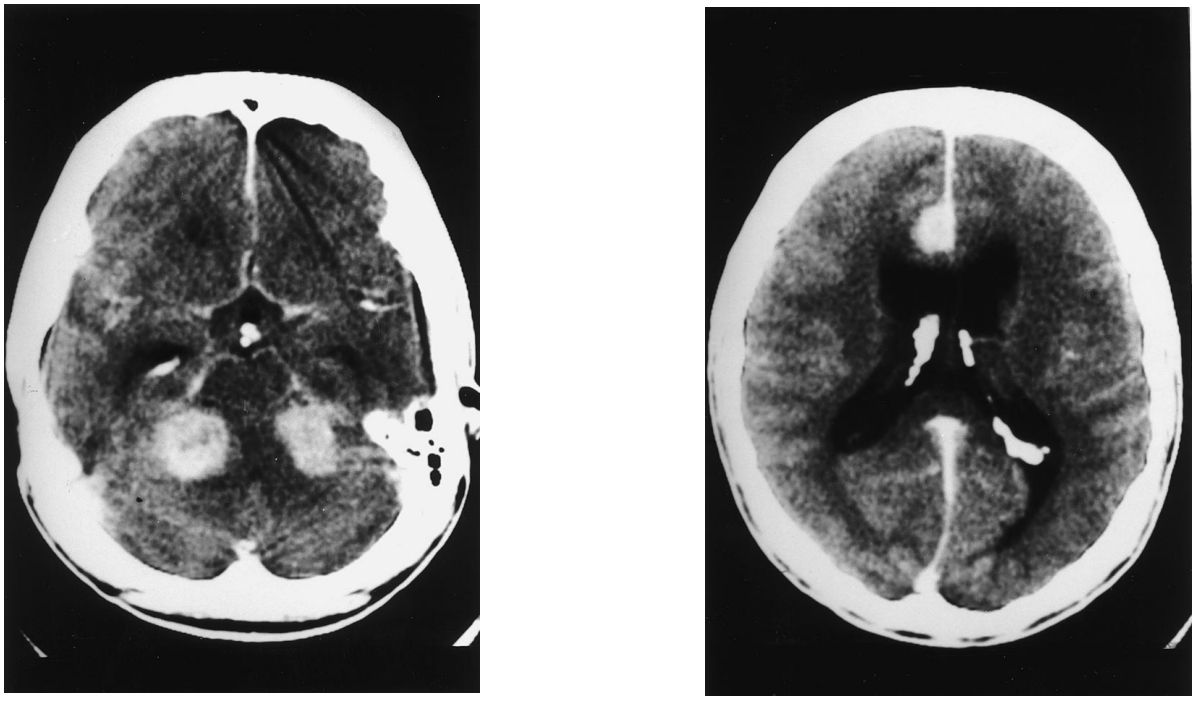

(*a*) (*b*)

Fig. 10 – A 21-year-old patient with NF-2. (*a*) CT following intravenous contrast medium shows bilateral vestibular schwannomas as enhancing cerebellopontine angle masses. (*b*) CT following intravenous contrast medium shows extensive choroid plexus calcification and a parafalcine meningioma.

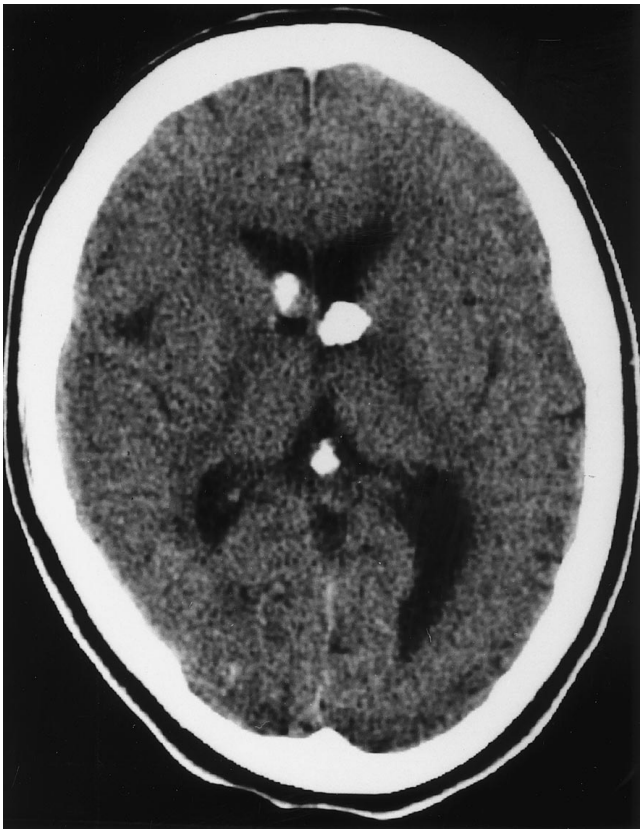

(*a*)

(*b*)

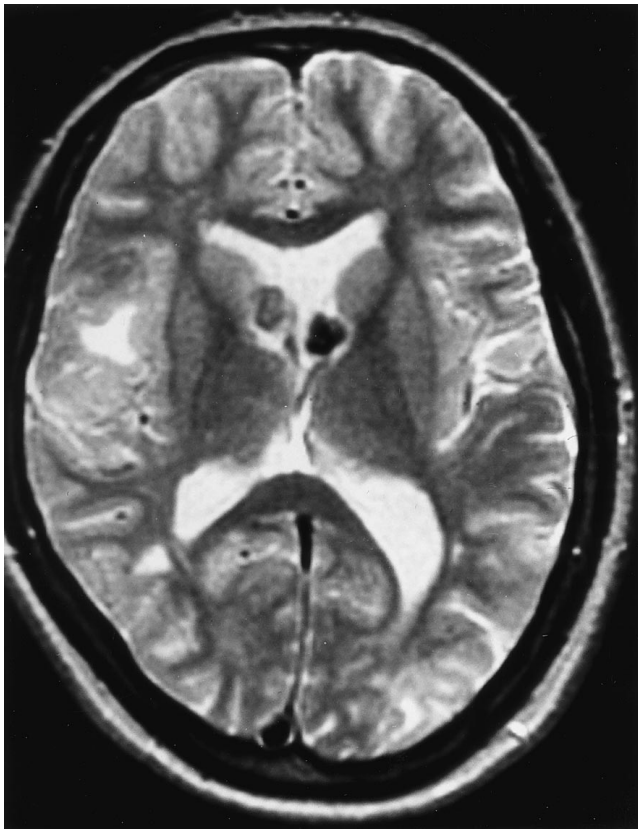

(*c*)

Fig. 11 – A 27-year-old patient with tuberous sclerosis. (*a*) Axial CT shows subependymal nodules (SEN). Most SEN calcify and at this stage are often better seen on CT as high attenuation nodules protruding into the ventricular surface. They rarely enhance on CT. Note the incidental pineal calcification. (*b*) Axial CT shows a SEN and a cortical tuber. Increasing numbers of these calcify with increasing age, although the proportion which do calcify has not been established. (*c*) MRI (T2-weighted axial) shows SEN with characteristic low signal and a cortical tuber. Cortical tubers vary in signal intensity according to patient age and myelination. In adults they show high signal on T2-weighted MRI, as in this figure. They show little signal change on T1-weighted MRI and rarely enhance. Enhancement is more commonly seen in neonates.

(*a*)

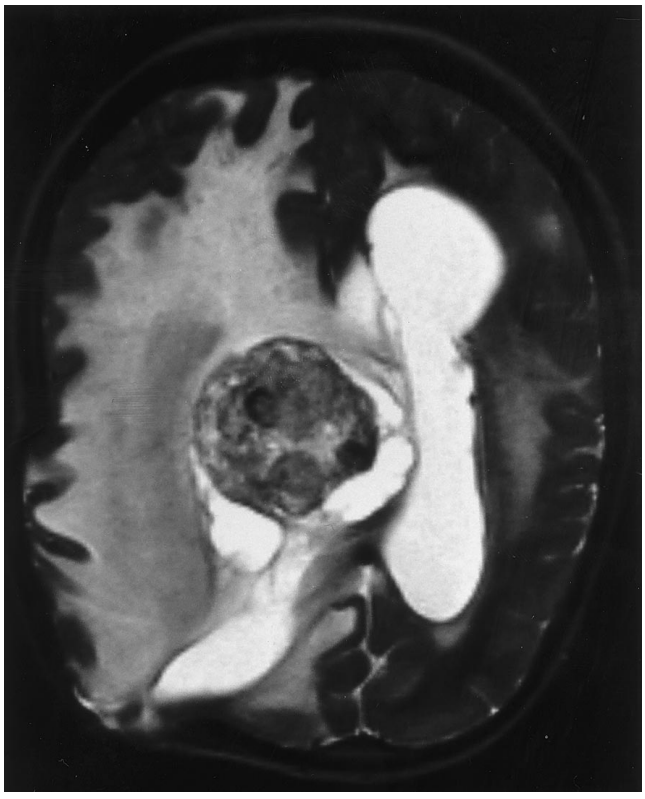

(*b*)

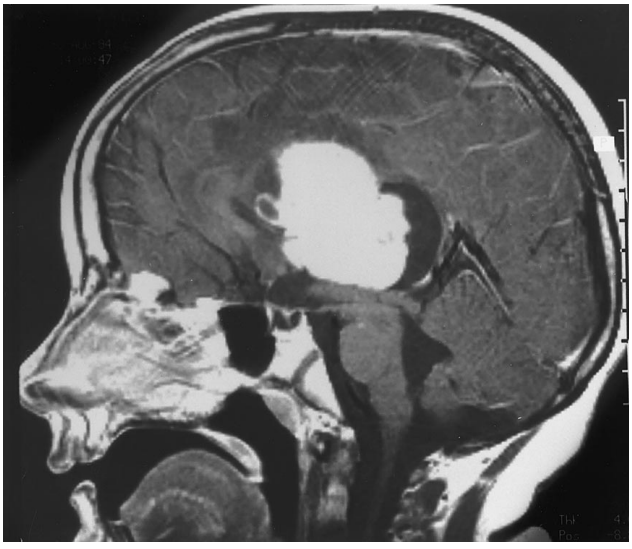

(*c*)

Fig. 12 – An 8-year-old patient with tuberous sclerosis. (*a*) Enhanced axial CT shows a giant cell astrocytoma, large amount of vasogenic oedema and a surgical defect of the skull. Note calcified SENs. These periventricular masses lie close to the foramen of Munro. They tend to enhance and in one-third of cases prominent flow voids are present. (*b*) MRI (T2-weighted axial) shows the mixed signal of the giant cell astrocytoma and prominent vasogenic oedema. (*c*) MRI (enhanced T1-weighted sagittal) shows the brightly enhancing giant cell astrocytoma.

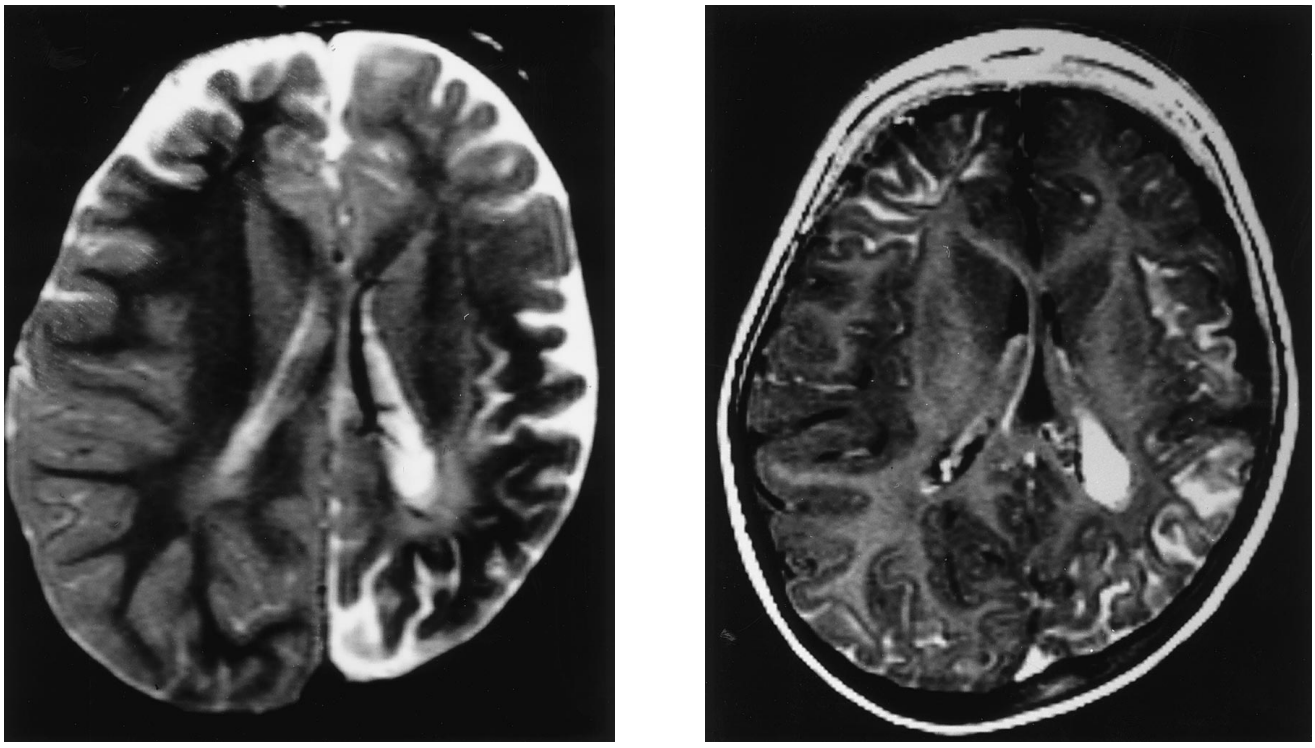

(*a*) (*b*)

Fig. 13 – A 5-month-old patient with Sturge Weber Syndrome. (*a*) MRI (T2-weighted axial) shows hemiatropy, (*b*) MRI (enhanced T1-weighted) shows high signal bilaterally in the leptomeninges and a large choroid plexus on the left.

Fig. 14 – A 46-year-old patient with Sturge Weber Syndrome. Axial CT shows cortical calcification. This dense gyriform calcification adjacent to abnormal meninges is best seen on CT but not before 1 year of age. The distribution is most often occipital (92%), parietal (61%), frontal (38%) and temporal (22%).

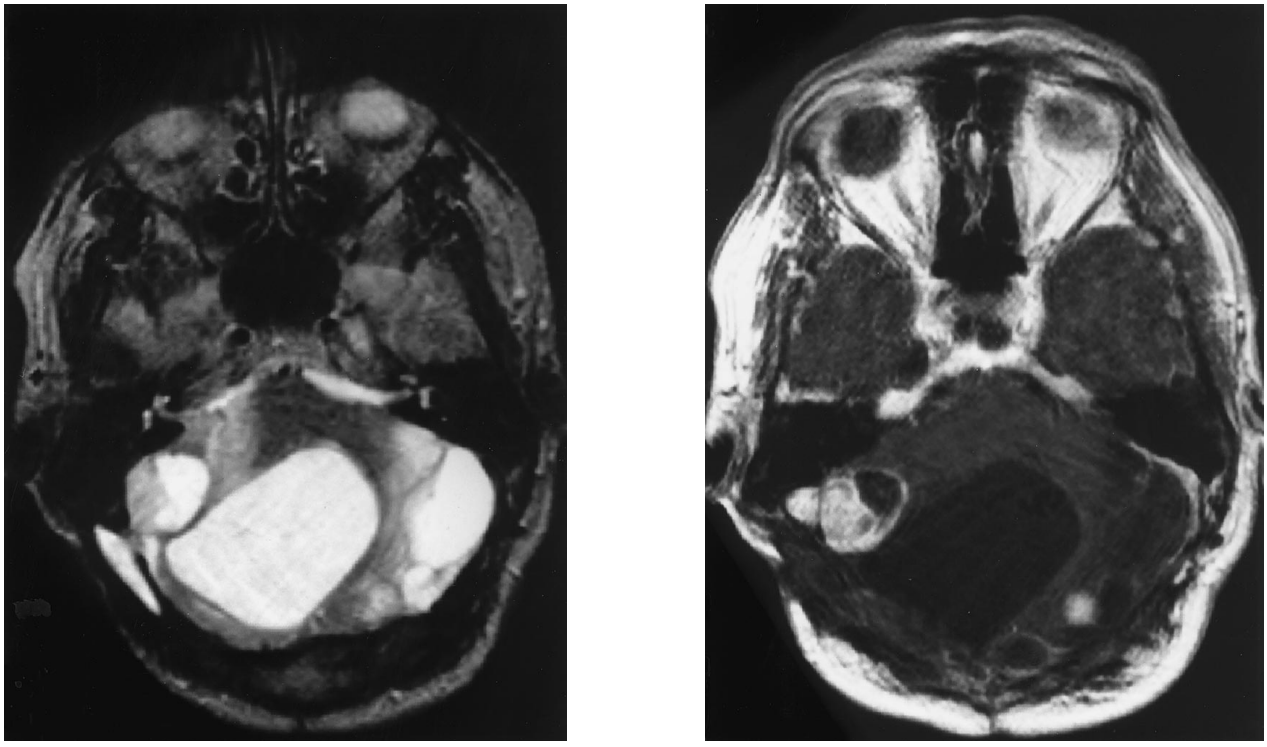

(*a*) (*b*)

Fig. 15 – A 53-year-old patient with Von Hippel Lindau Syndrome. (*a*) MRI (T2-weighted axial) shows multiple large cystic haemangioblastomas. A solid nodule is seen. (*b*) MRI (enhanced T1-weighted axial) shows the nodule enhancing avidly.

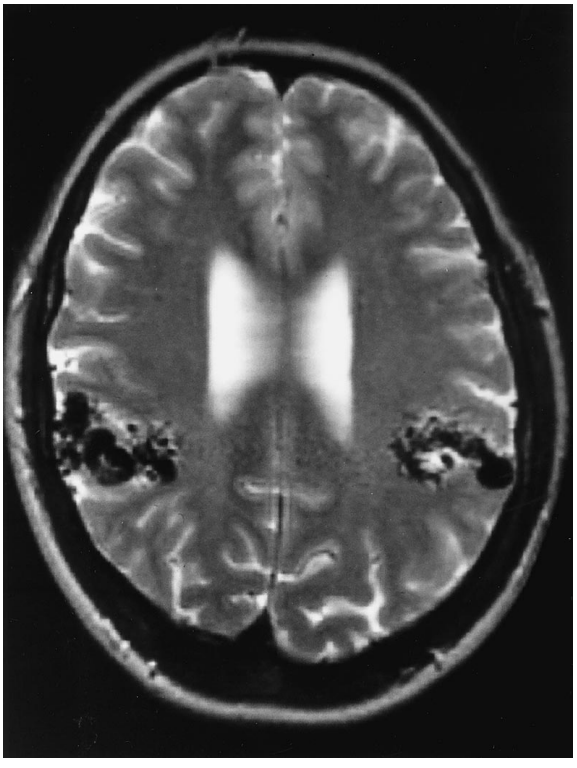

Fig. 16 – A 54-year-old patient with Wyburn-Mason Syndrome. MRI (T2-weighted axial) shows signal voids due to bilateral AVMs.

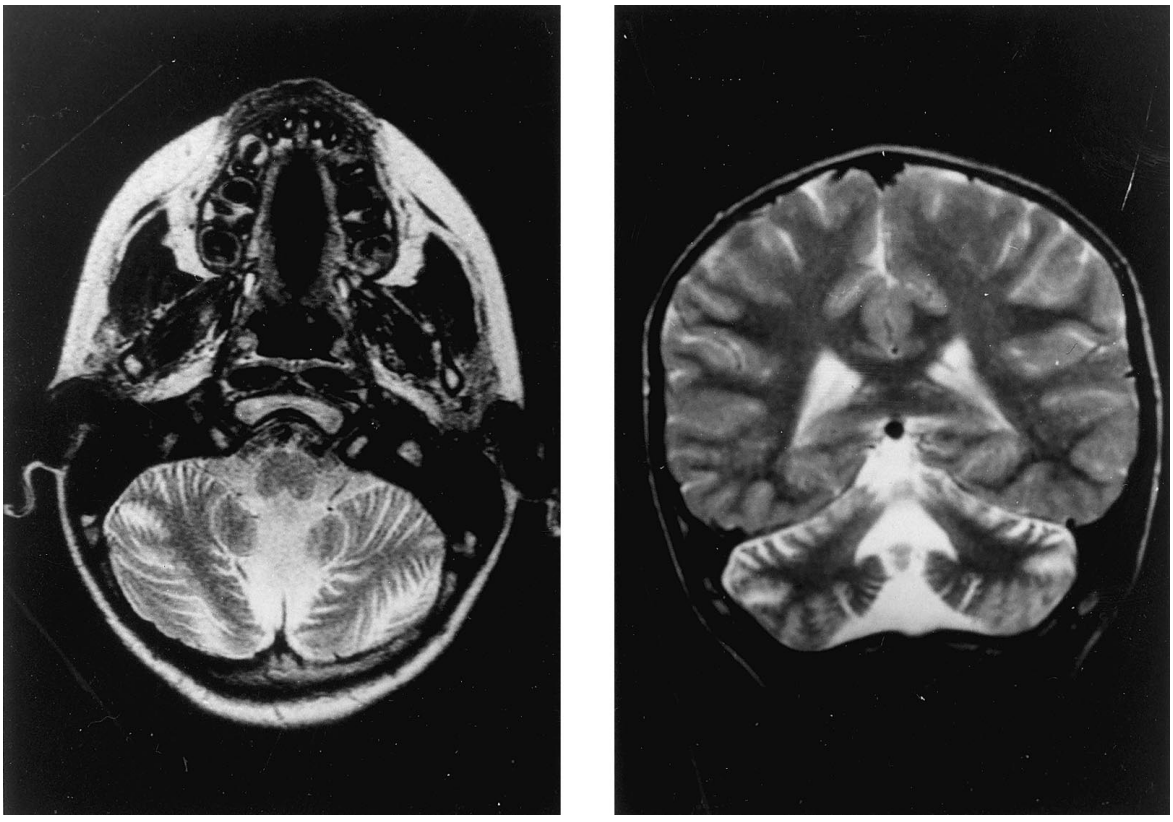

(*a*)

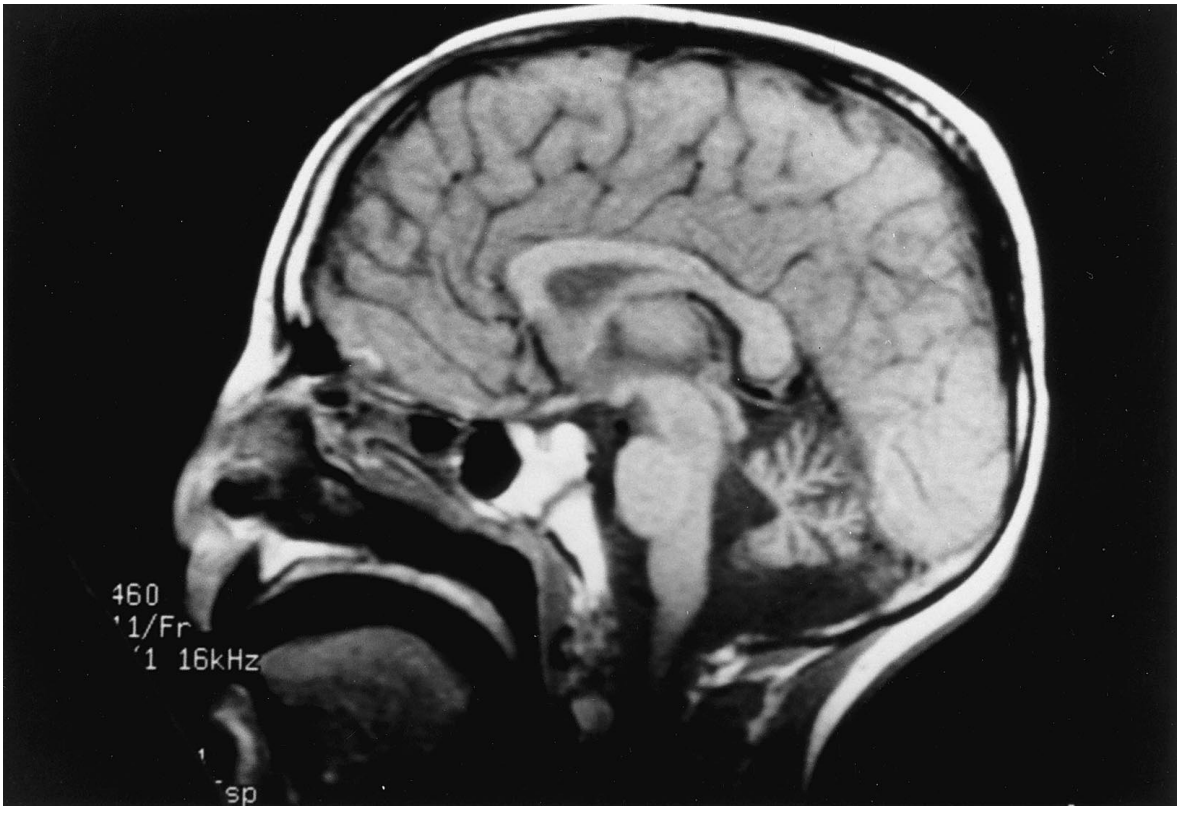

(*b*)

Fig. 17 – An 11-year-old patient with ataxia telangiectasia. (*a*) MRI (T2-weighted axial and coronal) shows marked cerebellar atrophy affecting mainly the anterior vermis, with atrophy of the olives and the dentate nucleus. (*b*) MRI (T1-weighted sagittal) shows cerebellar atrophy.

Table 3 – Diagnostic criteria for tuberous sclerosis are [8]:

Primary features
Facial angiofibromas
Multiple ungual fibromas
Cortical tuber (histologically confirmed)
Subependymal nodule or giant cell astrocytoma (histologically confirmed)
Multiple calcified supependymal nodules protruding into the ventricle (radiographic evidence)
Multiple retinal astrocytomas
Secondary features
Affected first-degree relative
Cardiac rhabdomyoma (histologic or radiographic confirmation)
Other retinal hamartoma or achromic patch
Noncalcified subependymal nodules (radiographic confirmation)
Shagreen patch
Forehead plaque
Pulmonary lymphangiomyomatosis (histological confirmation)
Renal angiomyolipoma (radiographic or histologic confirmation)
Renal cysts (histologic confirmation)
Tertiary features
Hypomelanotic macules
'Confetti' skin lesions
Renal cysts (radiographic evidence)
Randomly distributed enamel pits in deciduous and/or permanent teeth
Bone cysts (radiographic confirmation)
Hamartomatous rectal polyps (histologic confirmation)
Pulmonary lymphangiomyomatosis (radiographic evidence)
Cerebral white matter migration tracts or heterotopias (radiographic evidence)
Gingival fibromas
Hamartomas of other organs (histologic confirmation)
Infantile spasms
Definite TS – either one primary and two secondary features, or one secondary and two teriary features
Probable TS – either one secondary and one tertiary feature, or three tertiary features
Suspect TS – either one secondary or two tertiary features

Table 4 – Diagnostic criteria for Von Hippel-Lindau syndrome are [12]:

In the presence of a family history of a retinal or CNS haemangioblastoma either:
One haemangioblastoma
Or one visceral lesion such as a renal tumour; pancreatic cyst or tumour; phaeochromocytoma or papillary cystadenoma of the epididymis
In an isolated case where there is no clear family history:
Two or more haemangioblastomas
One haemangioblastoma and one visceral manifestation as listed above

lesions are associated with lesions in the CNS. 59% of cases have CNS lesions including cerebral atrophy, abnormalities of migration, gliosis and white matter involvement.

REFERENCES

1 Barkovich AJ. *Pediatric Neuroimaging*. 2nd edn. New York, Raven Press, 1995; 277–320.
2 Smirniotopoulos JG, Murphy FM. The phakomatoses. *Am J Neuroradiol* 1992;13:725–746.
3 National Institutes of Health Consensus Development Conference. *Arch Neurol* 1988;45:575–578.
4 Braffman BH, Bilaniuk LT, Zimmerman RA. MR for central nervous system neoplasia of the phakomatoses. *Semin Roentgenol* 1990;25:198–217.
5 Shy HH, Mirowitz SA, Wippold II. Neurofibromatosis: MR imaging findings involving the head and spine. *Am J Radiol* 1993;160:159–164.
6 Riccardi VM. Neurofibromatosis. *Neurol Clin* 1987;5:337–349.
7 Griffiths PD, Martland TR. Tuberous sclerosis complex: the role of neuroradiology. *Neuropediatrics* 1997;28:224–252.
8 Roach ES, Smith M, Huttenlocher P, Bhat M, Alcorn D, Hawley L. Diagnostic criteria: tuberous sclerosis complex. *J Child Neurol* 1992;7:221–223.
9 Shepard CW, Houser OW, Gomez MR. MR findings in tuberous sclerosis complex and correlation with seizure development and mental impairment. *Am J Neuroradiol* 1995;16: 145–155.
10 Griffiths PD. Sturge-Weber syndrome revisited: the role of neuroradiology. *Neuropediatrics* 1996;27:284–294.
11 Griffiths PD, Blaser S, Boodram MB, Armstrong D, Harwood-Nash D. Choroid plexus size in young children with Sturge-Weber Syndrome. *Am J Neuroradiol* 1996;17:175–180.
12 Choyke PL, Glenn GM, Walther MM, Patronas NJ, Lineham WM, Zbar B. Von Hippel-Lindau disease: genetic, clinical and imaging features. *Radiology* 1995;194:629–642.
13 Sato Y, Waziri M, Smith W, Frey E, Yuh W, Hanson J, Franken E. Hippel-Lindau disease: MR imaging. *Radiology* 1998;166:241–246.
14 Roach ES. Diagnosis and management of neurocutaneous syndromes. *Semin Neurol* 1988;1:83–96.